Annals of Physics 382 (2017) 160–169

Contents lists available at ScienceDirect

Annals of Physics

journal homepage: www.elsevier.com/locate/aop

New edge-centered photonic square lattices with flat bands

Da Zhang [a], Yiqi Zhang [a,b,*], Hua Zhong [a], Changbiao Li [a,b], Zhaoyang Zhang [a,b], Yanpeng Zhang [a,**], Milivoj R. Belić [c,**]

[a] Key Laboratory for Physical Electronics and Devices of the Ministry of Education & Shaanxi Key Lab of Information Photonic Technique, Xi'an Jiaotong University, Xi'an 710049, China
[b] Department of Applied Physics, School of Science, Xi'an Jiaotong University, Xi'an 710049, China
[c] Science Program, Texas A&M University at Qatar, P.O. Box 23874 Doha, Qatar

HIGHLIGHTS

- New edge-centered photonic square lattices with multiple flat bands are designed.
- Flat bands are obtained which are independent of the pseudomagnetic field.
- Strong localization is demonstrated if the flat-band mode is excited.
- Beams may oscillate, and the period depends on the difference of the flat bands.

ARTICLE INFO

Article history:
Received 28 December 2016
Accepted 30 April 2017
Available online 15 May 2017

Keywords:
Edge-centered lattice
Flat band
Localization

ABSTRACT

We report a new class of edge-centered photonic square lattices with multiple flat bands, and consider in detail two examples: the Lieb-5 and Lieb-7 lattices. In these lattices, there are 5 and 7 sites in the unit cell and in general, the number is restricted to odd integers. The number of flat bands m in the new Lieb lattices is related to the number of sites N in the unit cell by a simple formula $m = (N-1)/2$. The flat bands reported here are independent of the pseudomagnetic field. The properties of lattices with even and odd number of flat bands are different. We consider the localization of light in such Lieb lattices. If the input beam excites the flat-band mode, it will not diffract during propagation, owing to the strong mode localization. In the Lieb-7 lattice, the beam will also oscillate

* Corresponding author at: Key Laboratory for Physical Electronics and Devices of the Ministry of Education & Shaanxi Key Lab of Information Photonic Technique, Xi'an Jiaotong University, Xi'an 710049, China.
** Corresponding authors.
E-mail addresses: zhangyiqi@mail.xjtu.edu.cn (Y.Q. Zhang), ypzhang@mail.xjtu.edu.cn (Y.P. Zhang), milivoj.belic@qatar.tamu.edu (M.R. Belić).

http://dx.doi.org/10.1016/j.aop.2017.04.016

during propagation and still not diffract. The period of oscillation is determined by the energy difference between the two flat bands. This study provides a new platform for investigating light trapping, photonic topological insulators, and pseudospin-mediated vortex generation.

1. Introduction

A flat band – the bandwidth of which is zero – plays an essential role in studying strongly correlated phenomena, because the eigenstates of the flat band are highly degenerate [1]. By the same token, the flat band can significantly help in the realization of nondiffracting and localized states, because both the first-order and second-order derivatives of the band are zero. Indeed, the localized flat-band modes [2,3] and image transmission [4–6] based on the flat-band modes have been reported in the Lieb lattice [7–12] and the kagome lattice [13–16]. These lattices possess one flat band under the tight-binding approximation, when only the nearest-neighbor (NN) hopping is considered. Up to date, there is a variety of models reported that exhibit flat bands [17–23], among which the Lieb lattice is perhaps the simplest one. By the way, the flat band is also reported in some other interesting lattices, such as kagome lattice [24], star lattice [25], super-honeycomb lattice [26,27], to name a few. The Lieb lattice, which is not a Bravais lattice, has 3 sites in the unit cell and represents a kind of edge-centered square lattice. If one views the Lieb lattice as originating from the square lattice, a natural question arises: Can one artificially fabricate other kinds of edge-centered square lattices? For example, an edge-centered square lattice with 5 or 7 sites in the unit cell. This program is undertaken in this paper. Since there are 3 sites in the unit cell of a usual Lieb lattice, the edge-centered square lattices with 5 and 7 sites introduced here will be referred to as the Lieb-5 and Lieb-7 lattices; they represent novel members of the edge-centered square lattice family with interesting properties. The usual Lieb lattice would then be the Lieb-3 lattice. We believe that these new edge-centered lattices can be realized by the direct laser writing technique [28].

In this paper, we first investigate the dispersion relations (the band structure) of such edge-centered photonic square lattices, based on the tight-binding method. Interestingly, these lattices carry multiple flat bands. There are other models that support more than one flat band [29,30], but these flat bands cannot be obtained without the pseudomagnetic field [31]. The flat bands we find in the Lieb-5 and Lieb-7 lattices are independent of the pseudomagnetic field and only include the NN hopping [32], as it will be seen. In this sense, our lattice geometry that includes only the NN hopping is quite different from the other flat-band models reported in the previous literature. The number of flat bands m in our model is related to the number of sites N in the unit cell by a simple empirical formula, $m = (N - 1)/2$. Thus, for N odd one can have an even or an odd number of flat bands. In addition to many potential applications in image processing, telecommunication and sensing, and strongly correlated states, we believe that the study reported here provides a new lattice platform for investigating phenomena associated with the flat bands and related topics.

The organization of the paper is as follows. In Sections 2 and 3 we investigate the dispersion relation as well as the localization of light due to the flat-band modes of the Lieb-5 and Lieb-7 lattices. In Section 4, we conclude the paper.

2. Lieb-5 lattice

We consider the propagation of laser light in waveguide arrays arranged according to the edge-centered Lieb lattices. The simplest new Lieb-5 lattice array is displayed in Fig. 1(a), in which the lattice sites at the bottom form a unit cell and the period of the lattice is set to be 1. The propagation of light in such a waveguide array can be described by the paraxial wave equation, which has the same form as the standard Schrödinger equation, except that time is replaced by the propagation distance [28,33,34]. Thus, the evolution coordinate is the longitudinal coordinate z, instead of time.

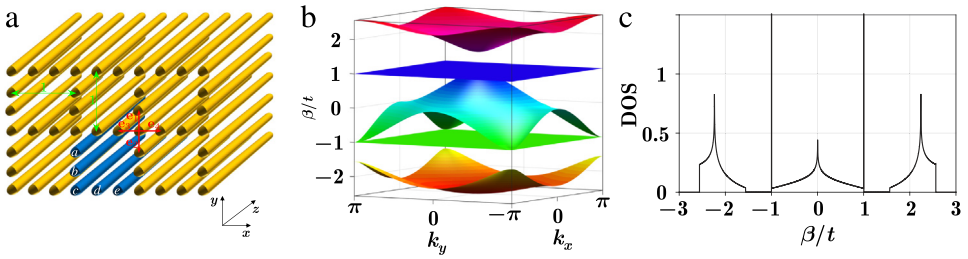

Fig. 1. Lieb-5 lattice array. (a) Photonic waveguide array arranged as an edge-centered square lattice with 5 sites in the unit cell, labeled as a, b, c, d, and e. The hopping unit vectors among NN sites are labeled by $\mathbf{e}_1$, $\mathbf{e}_2$, $\mathbf{e}_3$, and $\mathbf{e}_4$. (b) Dispersion relation. From top to bottom, the bands are $\beta_{1\sim5}$, respectively. (c) Density of states per unit cell as a function of the eigenvalues (in units of the hopping strength).

In the coupled mode regime, the propagation dynamics of light in this discrete model can be described by the discrete coupled Schrödinger equations [35]

$$i\frac{\partial a_m}{\partial z} = t\sum_{\boldsymbol{R}_m,\mathbf{e}_i}(b_m + c_m), \tag{1a}$$

$$i\frac{\partial b_m}{\partial z} = t\sum_{\boldsymbol{R}_m,\mathbf{e}_i}(a_m + c_m), \tag{1b}$$

$$i\frac{\partial c_m}{\partial z} = t\sum_{\boldsymbol{R}_m,\mathbf{e}_i}(a_m + b_m + d_m + e_m), \tag{1c}$$

$$i\frac{\partial d_m}{\partial z} = t\sum_{\boldsymbol{R}_m,\mathbf{e}_i}(c_m + e_m), \tag{1d}$$

$$i\frac{\partial e_m}{\partial z} = t\sum_{\boldsymbol{R}_m,\mathbf{e}_i}(c_m + d_m), \tag{1e}$$

where $\boldsymbol{R}_m$ is the position of the mth unit cell and $\mathbf{e}_i$ are the 4 vectors connecting the neighboring sites, as displayed in Fig. 1(a). We assume that the hopping among lattice points only happens between the NN sites, with t being the hopping strength. We are looking for the solutions to Eqs. (1a)–(1e) of the form [36]: $a_m = a_{\mathbf{k}}\exp[i(\beta z + \boldsymbol{R}_m\cdot\mathbf{k})]$, $b_m = b_{\mathbf{k}}\exp[i(\beta z + \boldsymbol{R}_m\cdot\mathbf{k})]$, $c_m = c_{\mathbf{k}}\exp[i(\beta z + \boldsymbol{R}_m\cdot\mathbf{k})]$, $d_m = d_{\mathbf{k}}\exp[i(\beta z + \boldsymbol{R}_m\cdot\mathbf{k})]$, $e_m = e_{\mathbf{k}}\exp[i(\beta z + \boldsymbol{R}_m\cdot\mathbf{k})]$, in which case one can rewrite Eqs. (1a)–(1e) in the matrix form, as an eigenvalue problem

$$H_{\mathrm{TB}}|\beta,\mathbf{k}\rangle = \beta|\beta,\mathbf{k}\rangle \tag{2}$$

with $|\beta,\mathbf{k}\rangle = [a_{\mathbf{k}}, b_{\mathbf{k}}, c_{\mathbf{k}}, d_{\mathbf{k}}, e_{\mathbf{k}}]^{\mathrm{T}}$ and H_{TB}, the tight-binding Hamiltonian of the system, being

$$H_{\mathrm{TB}} = -t\begin{bmatrix} 0 & H_y^* & H_y & 0 & 0 \\ H_y & 0 & H_y^* & 0 & 0 \\ H_y^* & H_y & 0 & H_x & H_x^* \\ 0 & 0 & H_x^* & 0 & H_x \\ 0 & 0 & H_x & H_x^* & 0 \end{bmatrix}, \tag{3}$$

where $H_x = \exp(ik_x/3)$ and $H_y = \exp(ik_y/3)$. Clearly, the matrix in Eq. (3) is equal to its own conjugate transpose, thus it is a Hermitian matrix, and the corresponding eigenvalues are completely

real. Diagonalizing H_{TB}, one obtains the eigenvalues $\beta_{1\sim5}$, as

$$\beta_1 = \sqrt[3]{-\frac{q}{2}+\sqrt{\left(\frac{q}{2}\right)^2+\left(\frac{p}{3}\right)^3}}+\sqrt[3]{-\frac{q}{2}-\sqrt{\left(\frac{q}{2}\right)^2+\left(\frac{p}{3}\right)^3}}, \tag{4a}$$

$$\beta_2 = t, \tag{4b}$$

$$\beta_3 = C_1\sqrt[3]{-\frac{q}{2}+\sqrt{\left(\frac{q}{2}\right)^2+\left(\frac{p}{3}\right)^3}}+C_2\sqrt[3]{-\frac{q}{2}-\sqrt{\left(\frac{q}{2}\right)^2+\left(\frac{p}{3}\right)^3}}, \tag{4c}$$

$$\beta_4 = -t, \tag{4d}$$

and

$$\beta_5 = C_2\sqrt[3]{-\frac{q}{2}+\sqrt{\left(\frac{q}{2}\right)^2+\left(\frac{p}{3}\right)^3}}+C_1\sqrt[3]{-\frac{q}{2}-\sqrt{\left(\frac{q}{2}\right)^2+\left(\frac{p}{3}\right)^3}}, \tag{4e}$$

with $C_1 = (-1-\sqrt{3}i)/2, C_2 = (-1+\sqrt{3}i)/2, p = -5t^2$ and $q = 2t^3[\cos(k_x)+\cos(k_y)]$. The eigenvalues in Eqs. (4b) and (4d) are independent of k_x and k_y, so they form flat bands in the first Brillouin zone. We would like to note that if higher order hopping, e.g. the hopping between next-nearest neighbor sites is considered, the completely flat bands will disappear. The eigenstates corresponding to the flat bands are

$$|\beta_2, \mathbf{k}\rangle = \left[-\frac{\exp(ik_y/3)}{-1+\exp(ik_y)}, -\frac{\exp(-ik_y/3)}{-1+\exp(-ik_y)}, 0, \frac{\exp(-ik_x/3)}{-1+\exp(-ik_x)}, \frac{\exp(ik_x/3)}{-1+\exp(ik_x)}\right]^{\mathrm{T}}, \tag{5a}$$

$$|\beta_4, \mathbf{k}\rangle = \left[-\frac{\exp(ik_y/3)}{1+\exp(ik_y)}, -\frac{\exp(-ik_y/3)}{1+\exp(-ik_y)}, 0, \frac{\exp(-ik_x/3)}{1+\exp(-ik_x)}, \frac{\exp(ik_x/3)}{1+\exp(ik_x)}\right]^{\mathrm{T}}, \tag{5b}$$

from which one can find that the amplitudes on sites a and b (as well as d and e) are complex conjugate of each other.

In Fig. 1(b), we show the band structure of the Lieb-5 lattice in the first Brillouin zone. One finds that, different from the usual Lieb lattice [9–11], there is no particle–hole symmetry for the states $|\beta_{1\sim5}, \mathbf{k}\rangle$, even though there are two flat bands. As an important quantity, the density of states (DOS) of a system is used to check how many states will be occupied per energy interval of a certain energy level. In Fig. 1(c), we display the DOS of the edge-centered photonic square lattice that corresponds to the band structure in Fig. 1(b). One finds that in the DOS diagram, the number of states increases sharply to a very large value from zero when the energy passes $\beta = \pm t$. The reason is clear — there are two band gaps which lead to zero DOS, but for a flat band, the states are numerous and degenerate, so the DOS increases sharply.

Next, we check the localization of light in the Lieb-5 lattice, due to flat-band modes. The propagation of light in such a lattice, based on Eqs. (1a)–(1e), is presented in Fig. 2. We assume that the input beam is an octupole that has eight peaks focused on sites a, b, d and e, as shown in Fig. 2(a). If the eight peaks are in-phase, then the beam undergoes discrete diffraction during propagation, as shown in Fig. 2(b), which presents the output intensity distribution of the beam.

On the other hand, if the eight peaks are out-of-phase, the fundamental flat-band mode will be excited, and the beam will remain localized and invariant during propagation. In Fig. 2(c), we show the output intensity distribution of the out-of-phase input with the corresponding input phase displayed in the left-bottom inset. As expected, the flat-band mode is excited, and the output beam intensity is the same as the input. In order to check the phase of each peak, we also display the interferogram of the output beam, by interfering the output beam with two tilted plane waves, as shown in the right two insets in Fig. 2(c). According to the interference stripes along the dashed lines, one finds that the initial out-of-phase structure is well preserved. If we change the phase distribution of the eight

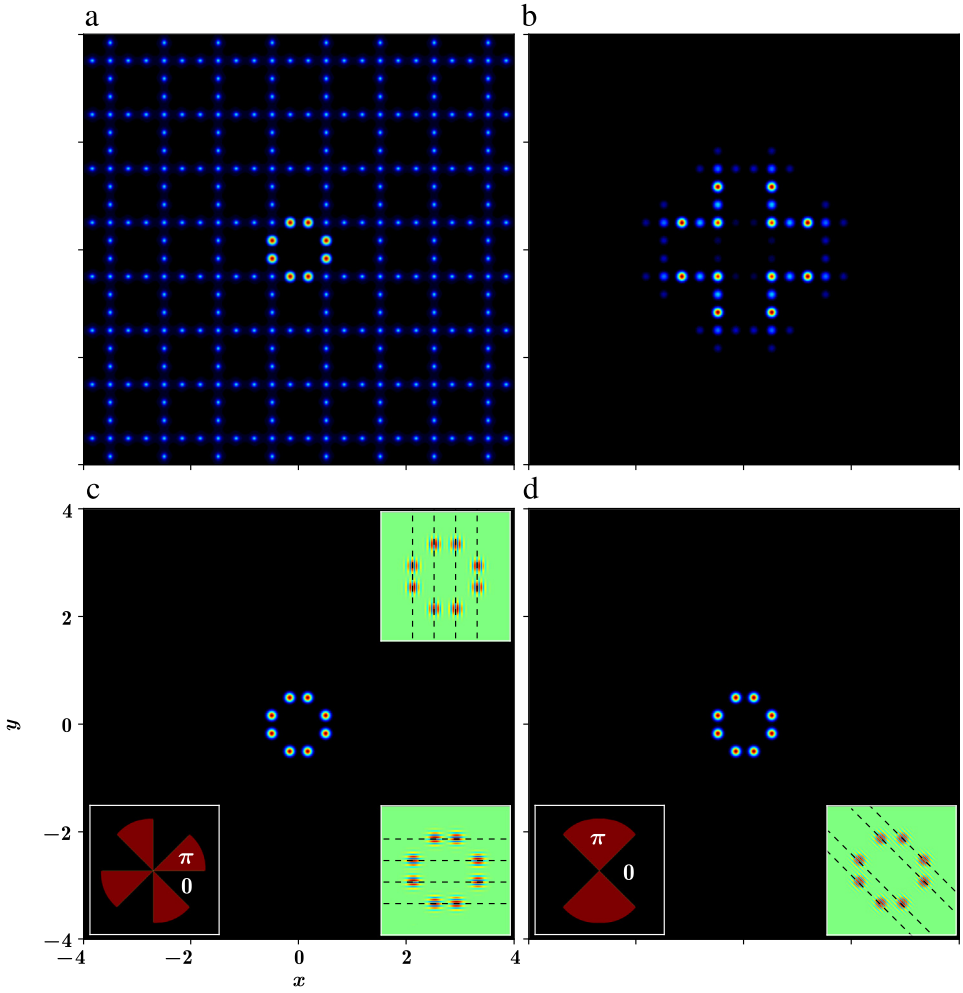

Fig. 2. Light localization due to the flat-band mode of the Lieb-5 lattice. (a) Intensity of the input that contains 8 peaks, which are exactly located at the sites, except the ones at the corners. (b) Discrete diffraction of the input if the peaks are in-phase. (c) Output intensity of the beam when the peaks are out-of-phase. Left-bottom inset: the phase of the input. Right top and bottom insets: interferograms of the output beam with tilted plane waves. (d) Figure setup is as in (c), but for the input with a different condition.

peaks of the input [the left-bottom inset in Fig. 2(d)], we find that the beam can still be well localized during propagation with the phase structure preserved, as shown in Fig. 2(d) and the right-bottom inset in this panel. From Fig. 2(c) and (d), one can advance the idea that both inputs with out-of-phase conditions can excite the flat-band modes efficiently, and will result in the localization of light propagating through the lattice.

3. Lieb-7 lattice

The Lieb-7 lattice is displayed in Fig. 3(a), and the period is still set to 1. Following the same method as for the Lieb-5 lattice, the Hamiltonian under the NN hopping approximation for the Lieb-7 lattice

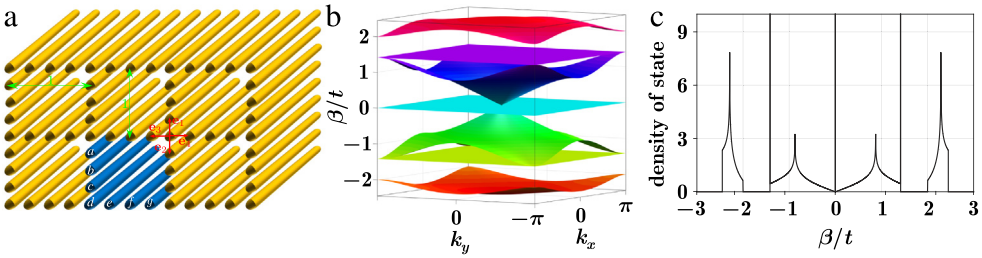

Fig. 3. Lieb-7 lattice waveguide array. Setup is the same as in Fig. 1.

can be written as

$$H_{\mathrm{TB}} = -t \begin{bmatrix} 0 & H_y^* & 0 & H_y & 0 & 0 & 0 \\ H_y & 0 & H_y^* & 0 & 0 & 0 & 0 \\ 0 & H_y & 0 & H_y^* & 0 & 0 & 0 \\ H_y^* & 0 & H_y & 0 & H_x & 0 & H_x^* \\ 0 & 0 & 0 & H_x^* & 0 & H_x & 0 \\ 0 & 0 & 0 & 0 & H_x^* & 0 & H_x \\ 0 & 0 & 0 & H_x & 0 & H_x^* & 0 \end{bmatrix}, \tag{6}$$

where $H_x = \exp(ik_x/4)$ and $H_y = \exp(ik_y/4)$, and the corresponding eigenvalues are

$$\beta_1 = \sqrt{3 + \sqrt{5 + 2\cos(k_x) + 2\cos(k_y)}}t, \tag{7a}$$

$$\beta_2 = \sqrt{2}t, \tag{7b}$$

$$\beta_3 = \sqrt{3 - \sqrt{5 + 2\cos(k_x) + 2\cos(k_y)}}t, \tag{7c}$$

$$\beta_4 = 0, \tag{7d}$$

$$\beta_5 = -\sqrt{3 - \sqrt{5 + 2\cos(k_x) + 2\cos(k_y)}}t, \tag{7e}$$

$$\beta_6 = -\sqrt{2}t, \tag{7f}$$

and

$$\beta_7 = -\sqrt{3 + \sqrt{5 + 2\cos(k_x) + 2\cos(k_y)}}t. \tag{7g}$$

Clearly, the Lieb-7 lattice possesses three flat bands $\beta_{2,4,6}$, as displayed in Fig. 3(b). Generally, one can obtain m flat bands, if there are $2m + 1$ sites in the unit cell for such novel kinds of the edge-centered square Lieb lattices. From the band structure, one finds that for each state $|\beta, \mathbf{k}\rangle$, there is a corresponding state $|-\beta, \mathbf{k}\rangle$. That is, there exists the particle–hole symmetry, which also exists in the usual Lieb lattice with only one flat band [9]. Thus, one should distinguish lattices with an even number of flat bands (such as Lieb-5 lattice) from the lattices with an odd number of flat bands (such as Lieb-7 lattice).

Another phenomenon that is similar to that in the usual Lieb lattice, is the existence of a single Dirac cone in the Lieb-7 lattice, which is intersected by the flat band β_4 and terminates at the other two flat bands $\beta_{2,6}$. It is worth mentioning that the Dirac cone is located at the center of the first Brillouin zone, which is different from the case of the usual Lieb lattice, where it is located at the corners of the first Brillouin zone. We should also mention that the appearance of Dirac cones at the center of the first Brillouin zone is determined by the degeneracy of the modes [37,38].

Corresponding to the flat bands, the eigenstates are

$$|\beta_{2,6}, \mathbf{k}\rangle = \Bigg[-\frac{\exp(ik_y/4)}{1+\exp(ik_y)},\ \pm\sqrt{2}\frac{\exp(ik_y/2)}{1+\exp(ik_y)},\ -\frac{\exp(-ik_y/4)}{1+\exp(-ik_y)},\ 0,\ \frac{\exp(-ik_x/4)}{1+\exp(-ik_x)},\ \mp\sqrt{2}\frac{\exp(ik_x/2)}{1+\exp(ik_x)},\ \frac{\exp(ik_x/4)}{1+\exp(ik_x)}\Bigg]^{\mathrm{T}}, \tag{8a}$$

$$|\beta_4, \mathbf{k}\rangle = \Bigg[-\frac{\exp(ik_y/4)}{-1+\exp(ik_y)},\ 0,\ -\frac{\exp(-ik_y/4)}{-1+\exp(-ik_y)},\ 0,\ \frac{\exp(-ik_x/4)}{-1+\exp(-ik_x)},\ 0,\ \frac{\exp(ik_x/4)}{-1+\exp(ik_x)}\Bigg]^{\mathrm{T}}, \tag{8b}$$

from which it is seen that the states on sites a and c (as well as e and g) are mutually complex conjugate. In Fig. 3(c), the DOS is presented, corresponding to the band structure in Fig. 3(b). In the DOS diagram, there are three sharp peaks (theoretically, the values are infinite) at the eigenvalues where the three flat bands are located.

Now, we turn to light localization in the Lieb-7 lattice, due to flat-band modes. We first launch a beam with eight peaks (an octupole) into the Lieb-7 lattice, such that the peaks excite sites a, c, e and g, as shown in Fig. 4(a1). If the eight peaks are neither in-phase nor out-of-phase, the beam will undergo discrete diffraction during propagation, as exhibited in Fig. 4(b1). We would like to note that the in-phase input may excite the mode of the Dirac cone, so instead of discrete diffraction, conical diffraction may occur. However, this topic is beyond the scope of the paper, and it will not be discussed any further. On the other hand, if the eight peaks of the beam profile have alternating signs, i.e., they are out-of-phase, the flat-band mode will be excited, and the beam will not diffract during propagation, as shown in Fig. 4(c1). There, the left-bottom inset shows the phase distribution of the input beam. Similar to Fig. 2(c), we also interfere the output beam with tilted plane waves, and the interferograms are displayed in the right-bottom insets in Fig. 4(c1). From the interferograms, one can see that the eight peaks are still out-of-phase. According to the eigenstates listed in Eqs. (8a) and (8b), one can recognize that the out-of-phase octupole input in Fig. 4(c1) excites the eigenstate $|\beta_4, \mathbf{k}\rangle$, which belongs to the flat band β_4.

Next, we will assume that the input beam is an octupole, but with the eight peaks not only not-in-phase, but also not-out-of-phase. Further, the peaks that excite sites a and c (as well as the peaks that excite sites e and g) are assumed in-phase, but the peaks at sites a (c) and e (g) are assumed out-of-phase, as shown in Fig. 4(a2) and the corresponding phase structure in the inset. One finds that the beam shows neither the discrete diffraction nor the strong localization during propagation, but it rather exhibits an oscillating behavior. The energy of the beam moves from sites a and c (e and g) to site b (c), to form a quadrupole, as shown in Fig. 4(b2), and then goes back to the octupole. This process proceeds periodically and circularly. If one records the maximum intensity $I_{\max}$ of the beam during propagation, the oscillation will be observed clearly, as presented in Fig. 4(c2), in which $I_{\max}$ is 1 at the initial place and 2 at $z = 10$, due to the change from an octupole to a quadrupole. The interferogram in the inset of Fig. 4(b2) shows that the phase structure is preserved, even though the intensity structure of the beam varies during propagation. Since the octupole and the quadrupole mutually transform, the same oscillating property can be also realized starting from a quadrupole input with alternating signs. Such a process is displayed in Fig. 4(a3)–(c3). Actually, Fig. 4(a2)–(c2) and (a3)–(c3) incarnate the reciprocity and the periodicity of this process.

It is worthwhile to understand why there is a periodic oscillation during propagation, and to determine the period. Since there is no discrete diffraction, the dispersive band modes are not excited. Considering the flat-band mode corresponding to β_4, it is excited by the out-of-phase octupole, hence the inputs in Fig. 4(a2)–(a4) can only excite the flat-band modes corresponding to $\beta_{2,6}$. Therefore, the oscillating property comes from the eigenstates $|\beta_{2,6}, \mathbf{k}\rangle$, as displayed in Eq. (8). Actually, one can find from the eigenstates $|\beta_{2,6}, \mathbf{k}\rangle$ that the sites a, b, c, e, f and g are all excited, and the amplitudes on sites b and f are $\sqrt{2}$ times of those on a, c, e and g. As a result, if the sites a, c, e and g are excited, sites b and f will be also excited, and *vice versa* — this mechanism leads to the periodic oscillation. Numerical

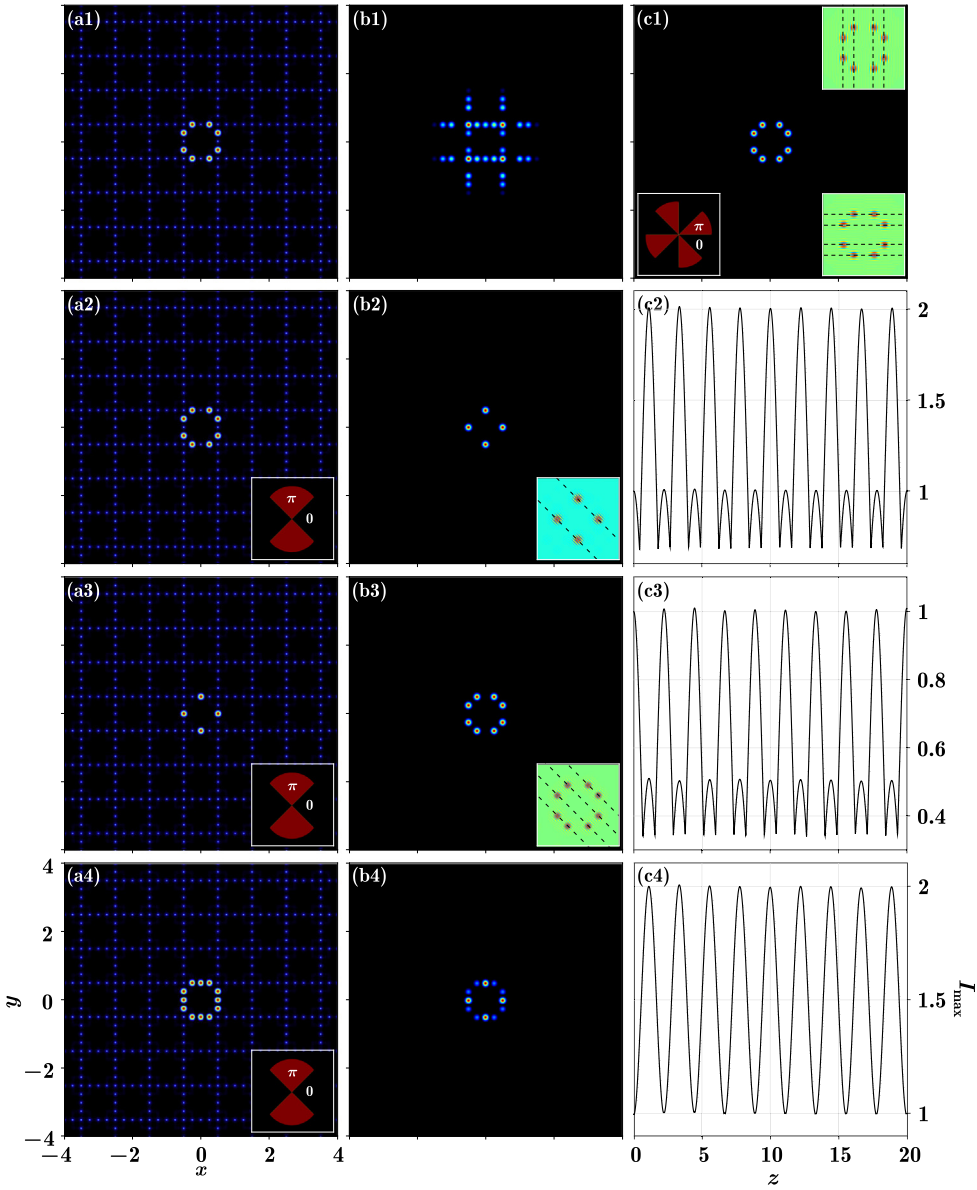

Fig. 4. Light localization due to the flat-band mode of the Lieb-7 lattice. (a1) Intensity of the input that contains 8 peaks which are exactly located at chosen sites. (b1) Discrete diffraction of the input if the peaks are neither in-phase nor out-of-phase. (c1) Output intensity of the beam if the peaks are out-of-phase. Left-bottom inset: phase of the input. Right top and bottom insets: interferograms of the output beam with tilted plane waves. (a2) Same as (a1), but with a different phase structure. Inset: phase of the input beam. (b2) Intensity of the beam at $z \approx 10$. Inset: interferogram of the output beam with a tilted plane wave. (c2) Maximum intensity of the beam versus propagation distance. (a3)–(c3) Same as (a2)–(c2), but with only sites b and f excited. (a4)–(c4) Same as (a2)–(c2), but for a superposed input that is composed of the inputs in (a2) and (a3). All panels except (c2)–(c4) share the same scales and dimensions.

simulations indeed demonstrate that the amplitudes in Fig. 4(b2) and (a3) are $\sqrt{2}$ times of those in Fig. 4(a2) and (b3), respectively. The physical reason for the oscillation is simultaneous excitation of

two flat bands with different energies [30]. Concerning the period, one should first determine the energy difference between the two flat bands $\Delta\beta = \beta_2 - \beta_6 = 2\sqrt{2}t$, and then find the period

$$D = \frac{2\pi}{\Delta\beta} = \frac{\pi}{\sqrt{2}t}. \tag{9}$$

Clearly, the period is associated with the hopping strength t, and the bigger the value of t, the smaller the period. In Fig. 4, we set $t = 1$, so there are about 9 periods over the distance of 20.

We would like to emphasize that the input can be arbitrarily constructed by the inputs used in Fig. 4, no matter which flat-band mode is excited. In other words, the freedom to observe the localization due to the flat band is much improved in comparison with earlier investigations. In Fig. 4(a4), we deliberately designed the input beam as a superposition of the inputs from Fig. 4(a2) and (a3). One finds that the intensity distribution of the corresponding output beam in Fig. 4(b4) is a superposition of the output intensity distributions from Fig. 4(b2) and (b3). The intensity difference between the octupole and the quadrupole in Fig. 4(b4) is due to the fact that the maximum intensity in Fig. 4(b2) is 4, while that in Fig. 4(b3) is 1. From this point of view, one could state that the excited flat-band modes are independent, and they will not affect each other during propagation. Because of the mutual transformation between the octupole and the quadrupole, the maximum intensity is not a simple sum of those in Fig. 4(c2) and (c3). As shown in Fig. 4(c4), the maximum intensity changes like a cosine curve with the propagation distance.

Last but not least, conical diffraction can be observed if light is launched into the site b and excites the modes around the Dirac cone [9]. As discussed above, there is no light located on the site b when the flat-band mode is excited, therefore, one may construct an input, based on which the flat-band modes and the Dirac cone modes are excited simultaneously. However, in this paper we omit the discussion of this aspect of beam propagation in the edge-centered Lieb lattices.

4. Conclusion

In summary, we have constructed two new kinds of edge-centered photonic square lattices — the Lieb-5 and Lieb-7 lattices, which possess even and odd number of flat bands. They belong to the family of edge-centered Lieb lattices with different number of sites in the unit cell. Similar to previous investigations, the flat-band modes are strongly localized when they are excited during propagation. On the other hand, different from previous investigations, such flat-band modes may exhibit oscillating property during propagation, which has never been observed before. By choosing certain flat-band modes to describe the beam input, complicated image transmission can be achieved. Our investigation points to potential applications in areas where flat bands can be applied, and in addition provides a new platform for investigating and understanding the phenomena connected with flat bands, such as light trapping. We also believe that the edge-centered square lattices may also have potential in studying photonic topological insulators (by breaking the time-reversal symmetry) and pseudospin-mediated vortex generation.

Acknowledgments

This work was supported by China Postdoctoral Science Foundation (2016M600777, 2016M590935, 2016M600777), the National Natural Science Foundation of China (11474228, 61605154), and Qatar National Research Fund (NPRP 6-021-1-005).

References

[1] K. Sun, Z. Gu, H. Katsura, S. Das Sarma, Phys. Rev. Lett. 106 (2011) 236803.
[2] R.A. Vicencio, C. Cantillano, L. Morales-Inostroza, B. Real, C. Mejía-Cortés, S. Weimann, A. Szameit, M.I. Molina, Phys. Rev. Lett. 114 (2015) 245503.
[3] S. Mukherjee, A. Spracklen, D. Choudhury, N. Goldman, P. Öhberg, E. Andersson, R.R. Thomson, Phys. Rev. Lett. 114 (2015) 245504.
[4] S. Xia, Y. Hu, D. Song, Y. Zong, L. Tang, Z. Chen, Opt. Lett. 41 (2016) 1435–1438.
[5] R.A. Vicencio, C. Mejía-Cortés, J. Opt. 16 (2014) 015706.

[6] Y. Zong, S. Xia, L. Tang, D. Song, Y. Hu, Y. Pei, J. Su, Y. Li, Z. Chen, Opt. Express 24 (2016) 8877–8885.
[7] V. Apaja, M. Hyrkäs, M. Manninen, Phys. Rev. A 82 (2010) 041402.
[8] R. Shen, L.B. Shao, B. Wang, D.Y. Xing, Phys. Rev. B 81 (2010) 041410.
[9] D. Leykam, O. Bahat-Treidel, A.S. Desyatnikov, Phys. Rev. A 86 (2012) 031805.
[10] M. Niță, B. Ostahie, A. Aldea, Phys. Rev. B 87 (2013) 125428.
[11] D. Guzmán-Silva, C. Mejía-Cortés, M.A. Bandres, M.C. Rechtsman, S. Weimann, S. Nolte, M. Segev, A. Szameit, R.A. Vicencio, New J. Phys. 16 (2014) 063061.
[12] Y.Q. Zhang, X. Liu, M. Belić, W.P. Zhong, C.B. Li, H.X. Chen, Y.P. Zhang, Rom. Rep. Phys. 68 (2016) 230–240.
[13] J.L. Atwood, Nature Mater. 1 (2002) 91–92.
[14] M. Boguslawski, P. Rose, C. Denz, Appl. Phys. Lett. 98 (2011) 061111.
[15] G.-B. Jo, J. Guzman, C.K. Thomas, P. Hosur, A. Vishwanath, D.M. Stamper-Kurn, Phys. Rev. Lett. 108 (2012) 045305.
[16] Y. Nakata, T. Okada, T. Nakanishi, M. Kitano, Phys. Rev. B 85 (2012) 205128.
[17] S. Deng, A. Simon, J. Köhler, J. Solid State Chem. (ISSN: 0022-4596) 176 (2003) 412–416.
[18] C. Wu, D. Bergman, L. Balents, S. Das Sarma, Phys. Rev. Lett. 99 (2007) 070401.
[19] A. Crespi, G. Corrielli, G.D. Valle, R. Osellame, S. Longhi, New J. Phys. 15 (2013) 013012.
[20] T. Jacqmin, I. Carusotto, I. Sagnes, M. Abbarchi, D.D. Solnyshkov, G. Malpuech, E. Galopin, A. Lemaître, J. Bloch, A. Amo, Phys. Rev. Lett. 112 (2014) 116402.
[21] Y.Q. Zhang, Z.K. Wu, M.R. Belić, H.B. Zheng, Z.G. Wang, M. Xiao, Y.P. Zhang, Laser Photonics Rev. 9 (2015) 331–338.
[22] S. Mukherjee, R.R. Thomson, Opt. Lett. 40 (2015) 5443–5446.
[23] S. Weimann, L. Morales-Inostroza, B. Real, C. Cantillano, A. Szameit, R.A. Vicencio, Opt. Lett. 41 (2016) 2414–2417.
[24] H.-M. Guo, M. Franz, Phys. Rev. B 80 (2009) 113102.
[25] W.-C. Chen, R. Liu, Y.-F. Wang, C.-D. Gong, Phys. Rev. B 86 (2012) 085311.
[26] Z. Lan, N. Goldman, P. Öhberg, Phys. Rev. B 85 (2012) 155451.
[27] H. Zhong, Y.Q. Zhang, Y. Zhu, D. Zhang, C.B. Li, Y.P. Zhang, F.L. Li, M.R. Belić, M. Xiao, Ann. Phys. (Berlin) (2017) 1600258 1600258.
[28] A. Szameit, S. Nolte, J. Phys. B: At. Mol. Opt. Phys. 43 (2010) 163001.
[29] J. Vidal, B. Douçot, R. Mosseri, P. Butaud, Phys. Rev. Lett. 85 (2000) 3906–3909.
[30] S. Longhi, Opt. Lett. 39 (2014) 5892–5895.
[31] M.C. Rechtsman, J.M. Zeuner, A. Tünnermann, S. Nolte, M. Segev, A. Szameit, Nature Photon. 7 (2013) 153–158.
[32] H. Tasaki, Comm. Math. Phys. (ISSN: 1432-0916) 242 (3) (2003) 445–472.
[33] M.C. Rechtsman, J.M. Zeuner, Y. Plotnik, Y. Lumer, D. Podolsky, F. Dreisow, S. Nolte, M. Segev, A. Szameit, Nature 496 (2013) 196–200.
[34] L.J. Maczewsky, J.M. Zeuner, S. Nolte, A. Szameit, Observation of photonic anomalous floquet topological insulators, Nat. Commun. 8 (2017) 13756.
[35] M.J. Ablowitz, Y. Zhu, Phys. Rev. A 82 (2010) 013840.
[36] A. Szameit, M.C. Rechtsman, O. Bahat-Treidel, M. Segev, Phys. Rev. A 84 (2011) 021806.
[37] J. Mei, Y. Wu, C.T. Chan, Z.-Q. Zhang, Phys. Rev. B 86 (2012) 035141.
[38] K. Sakoda, Opt. Express 20 (22) (2012) 25181–25194.